A Reconfigurable Single-Stage Three-Phase Electric Vehicle DC Fast Charger Compatible With Both 400V and 800V Automotive Battery Packs

Mojtaba Forouzesh, Yan-Fei Liu, Paresh C. Sen
Queen's University
Department of Electrical and Computer Engineering
Kingston, ON, Canada
E-Mail: m.forouzesh@queensu.ca, yanfei.liu@queensu.ca, senp@queensu.ca
URL: https://www.ece.queensu.ca/research/labs/power-group.html

Keywords

«Electric vehicle (EV)», «Charging infrastructure for EVs», «AC-DC converter», «Power factor correction», «Resonant converter».

Abstract

A novel three-phase Electric Vehicle (EV) DC fast charger with a wide output voltage range is proposed in this paper. One of the main features of the proposed EV charger is that it can provide a wide output voltage range (i.e., 250 V to 850 V) using low voltage rating mainstream switches/diodes (i.e., 650 V). The proposed EV charger takes advantage of Inductor-Inductor-Capacitor (LLC) resonant tanks for each phase allowing soft-switching performance for all switches so the major power loss will be only conduction loss. Consequently, by operating at a high switching frequency the size of passive components can be reduced leading to a high-power density. Moreover, as the AC to DC conversion is being realized in an isolated single-stage approach, the total conversion efficiency for the proposed EV charger is higher than conventional two-stage EV chargers. The analysis of the power circuit design and control of the proposed EV fast charger is provided in the paper for both 400 V and 800 V automotive battery systems. Moreover, the performance is verified by computer simulation results and experimental results of a 1.5 kW laboratory prototype.

Introduction

In recent decades a lot of attention is paid to renewable energy technologies due to the increased greenhouse emissions and other environmental concerns [1]. One of the main contributors to the emission of CO2 is transportation which is mainly consisted of internal combustion engine vehicles. To overcome this issue, it is widely accepted that more efficient and affordable Electric Vehicles (EVs) should be replaced with existing vehicles. Therefore, EV power train technologies have been the topic of a lot of research studies in the past decade [2] and [3]. Most recent EVs use a 400 V powertrain system which is well established and standardized through the years. From the advent of EVs, one of the early concerns about them was their limited driving range, which is being fulfilled by adding to the capacity of the long-range EV battery packs. The latter brings forward another challenge which is the long recharging time of a depleted high-capacity battery pack. To address the high power charging challenge, DC fast chargers that have been classified as the level 3 charging method for EV charging stations are meant to provide high power DC voltage directly to the EV battery [4].

The conventional method for DC fast charger is based on a two-stage approach to achieve the required specifications [5], with a direct three-phase AC-DC converter like Vienna rectifier at the grid side to achieve Power Factor Correction (PFC) [6]. In the second stage, soft-switching DC-DC converters like phase-shifted full-bridge converters or LLC resonant converters are preferred to provide voltage isolation and regulation while achieving high efficiency in DC-to-DC conversion [7] and [8]. To improve efficiency, interleaving multiphase DC-DC converters is a necessity for high-power chargers, which can be a challenging task for resonant converters [9]. Because of using two cascaded stages in the conventional method, the total AC-to-DC conversion efficiency is usually limited to below 96% and the power density is also suffering due to many active and passive components.

In recent years, single-stage EV chargers are becoming attractive due to their ability to improve both efficiency and power density [10]-[12]. In [10] a DAB-based direct three-phase AC-DC converter is proposed using a matrix converter at the primary of the transformer with back-to-back switches. In [11], a phase-modular three-phase AC-DC converter is proposed for EV battery charging applications using Cuk converter modules. This converter lacks soft-switching and suffers high current stress making it less attractive for high-power applications. In [12], a soft-switching phase-modular three-phase AC-DC converter is proposed for EV battery charging. The efficiency is low as a result of large current ripples due to using DCM boost inductors to obtain inherent PFC.

In the past decades, most of the literature only discussed EV chargers for a 400 V system while an 800 V system is beginning to take more attention in recent years [13]-[15]. In [16], a single-stage single-phase EV charger based on a bridgeless boost PFC rectifier and a three-level CLL resonant converter with three winding transformers is proposed. The secondary and tertiary windings of the transformer are connected in series with a coupled inductor to provide 800V at the battery side. The output voltage of this converter has a double line frequency ripple and hence needs a ripple cancellation method. In [17] a single-stage three-phase EV charger is proposed based on a phase-modular approach using a dual active bridge converter. Although it is mentioned that the proposed charger is suitable for a wide output voltage range, sufficient analysis and verification are not provided.

Since the 800 V EV battery that was first proposed by Porsche and now is being used by other automakers consists of two series-connected modules with equal cells [13], a Battery Selection Circuit (BSC) is proposed in [18] to be added at the output of exiting EV chargers allowing both 400 V and 800 V battery charging. The proposed BSC charges two 400 V battery modules interchangeably so the semiconductors are all rated for a 400 V system. However, this circuit introduces additional loss when charging a 400 V EV battery pack and it requires additional battery management systems at the charger side for safety reasons. In [19], a two-stage three-phase EV charger is proposed that is suitable for both 400 V and 800 V batteries. A direct three-phase Boost PFC is used at the input followed by a three-active bridge DC-DC converter with two transformers. The output of the transformers is connected in a reconfigurable fashion so both output charging voltage ranges can be met. The stress of components is large as a direct three-phase approach is used and the efficiency is not high enough due to the dual power processing stages.

In this paper, a novel single-stage three-phase EV charger is proposed with a wide output voltage range. Fig.1 illustrates a general block diagram of the proposed EV charger with reconfigurable output that can be used with both 400 V and 800 V EV battery voltages (V_B). Moreover, the proposed EV charger has a phase-modular structure using LLC PFC converter modules [20], which allows achieving soft-switching over a wide output voltage range. Furthermore, unlike most other power electronics converters suitable for the EV 800 V system, in the proposed EV charger there is no need for 1200 V SiC devices, and only 650 V switches/diodes are used. The proposed converter is introduced and analyzed in the next section. Then, simulation and experimental results are provided to verify the performance. Finally, the paper is concluded in the last section.

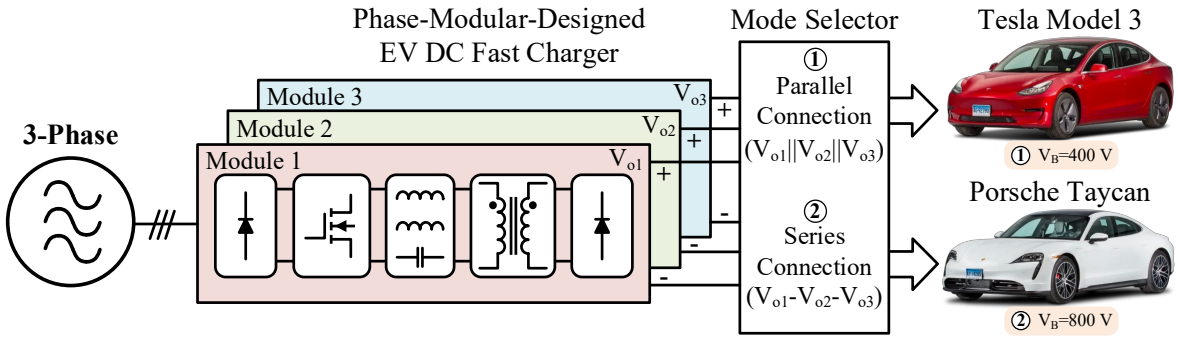

Fig. 1. Block diagram illustration of the proposed EV charger with reconfigurable output.

The proposed single-stage three-phase EV charger

Fig. 2 illustrates the proposed single-stage three-phase EV charger with reconfigurable output. When two double pole relays are in position 1 the output is set for 400 V battery systems ($V_o{}^{400} = V_{o1} = V_{o2} = V_{o3}$) and when the relays are in position 2 the output is set for 800 V battery systems ($V_o{}^{800} = V_{o1} + V_{o2} + V_{o3}$). The proposed three-phase charger has a phase-modular structure, so the maximum stress is distributed among components leading to high reliability, high efficiency, and low cost. Each phase is consisted of an LLC converter module to take advantage of Zero Voltage Switching (ZVS) and Zero Current Switching (ZCS) for all the switching devices. The latter allows high switching frequency implementation in the proposed three-phase rectifier leading to a high power density. The PFC is achieved by changing the switching frequency of each phase with respect to the line AC voltages. In this way, using a low-quality factor (Q) resonant tank design allows for achieving high voltage gains around the parallel resonant frequency (f_p), which is required around the line Voltage Zero Crossing (VZC) area. Moreover, the voltage gain requirement around the peak line voltage is minimum and usually is set to be around the series resonant frequency (f_s) keeping the operation in the below resonant area to take advantage of ZCS for the diodes.

Considering that the switching frequency is much higher than the AC line frequency, there is negligible high-frequency current flowing into the output capacitors. Then, the rectified output current of each phase ($i_{o1,2,3}$) can be represented by its fluctuating average value, which can be written based on the instantaneous input voltages ($v_a(t), v_b(t), v_c(t)$) and input currents ($i_a(t), i_b(t), i_c(t)$) of a balanced three-phase system with 120° phase displacement connected to a unity power factor correction lossless three-phase circuit. Then in a balanced three-phase system, the fluctuating part of the voltage and current get canceled in the output. Hence, the battery voltage and current for both output modes can be written based on the average voltages and currents and the Root Mean Square (RMS) value of the AC voltages (V_{ac}) and currents (I_{ac}) in the following forms.

$$V_B{}^{400} = V_{o1} = V_{o2} = V_{o3}\,, I_B{}^{400} = I_{o1} + I_{o2} + I_{o3} = 3 \times \frac{V_{ac} I_{ac}}{V_B{}^{400}} \tag{1}$$

$$V_B{}^{800} = V_{o1} + V_{o2} + V_{o3} = 3 \times \frac{V_{ac} I_{ac}}{I_B{}^{800}}\,, I_B{}^{800} = I_{o1} = I_{o2} = I_{o3} \tag{2}$$

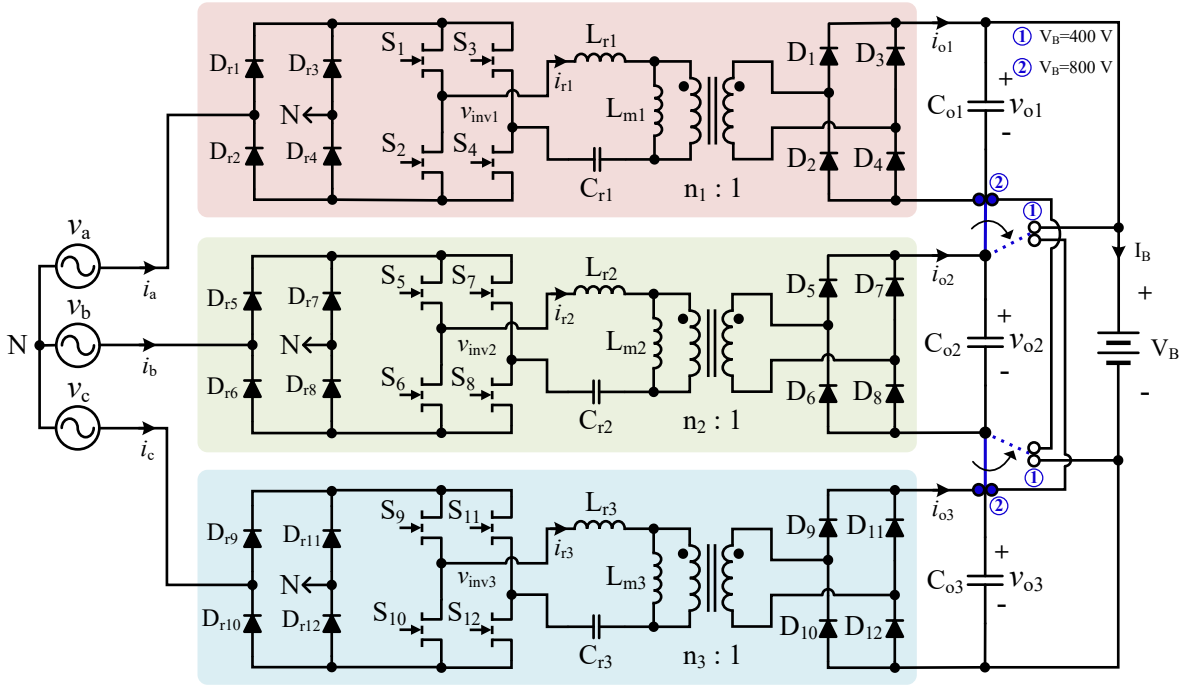

Fig. 2. The proposed single-stage three-phase EV charger with reconfigurable output.

The equivalent model of the three-phase AC-DC LLC converter in both output configuration modes is shown in Fig. 3. The input of each LLC resonant tank is a square wave voltage coming from the inverter bridge that is dependent on the line angle and its initial value, θ and θ_0, respectively. In a balanced three-phase system with 120° phase displacement, θ_0 is equal to zero for phase 1, it is equal to -120° for Phase 2, and it is equal to +120° for phase 3. The equivalent load resistance transferred to the primary side of the transformer of each phase can be written in terms of fluctuating output power over the line cycle that is equal to the input power for a lossless circuit (i.e., $p_{in}(\theta+\theta_0) = p_o(\theta+\theta_0)$).

$$p_{o(1,2,3)}(\theta+\theta_0) = 2\times\sin^2(\theta+\theta_0)\times P_{o(1,2,3)} = 2\times\sin^2(\theta+\theta_0)\times\frac{v_{oe(1,2,3)}^2}{R_{oe(1,2,3)\_FL}} \tag{3}$$

$$R_{oe(1,2,3)\_FL} = \frac{8\times n_{(1,2,3)}^2}{\pi^2}\times R_{L(1,2,3)\_FL} = \frac{8\times n_{(1,2,3)}^2}{\pi^2}\times\frac{V_{o(1,2,3)}}{I_{o(1,2,3)\_FL}} \tag{4}$$

$$\begin{aligned} R_{o(1,2,3)}(\theta+\theta_0) &= \frac{v_{oe(1,2,3)}^2}{p_{o(1,2,3)}(\theta+\theta_0)} = \frac{R_{oe(1,2,3)\_FL}}{2\sin^2(\theta+\theta_0)} = \frac{4\times n_{(1,2,3)}^2}{\pi^2\sin^2(\theta+\theta_0)}\times R_{L(1,2,3)\_FL} \\ &= \frac{4\times n_{(1,2,3)}^2}{\pi^2\sin^2(\theta+\theta_0)}\times\frac{V_{o(1,2,3)}}{I_{o(1,2,3)\_FL}} \end{aligned} \tag{5}$$

where $R_{oe(1,2,3)\_FL}$ is the equivalent load resistance transferred to the primary side of the transformers, $R_{L(1,2,3)\_FL}$ is the output load resistance of each phase, and $I_{o(1,2,3)\_FL}$ is the output load current of each phase when operating at full output power ($P_{o(1,2,3)}$).

Then with a balanced power distribution between the three-phase modules ($P_{o(1,2,3)} = P_o/3$), the total equivalent load resistance at the primary of the transformers for the three-phase system is not dependent on the line cycle angle as the AC line fluctuation gets canceled in the output in a balanced system.

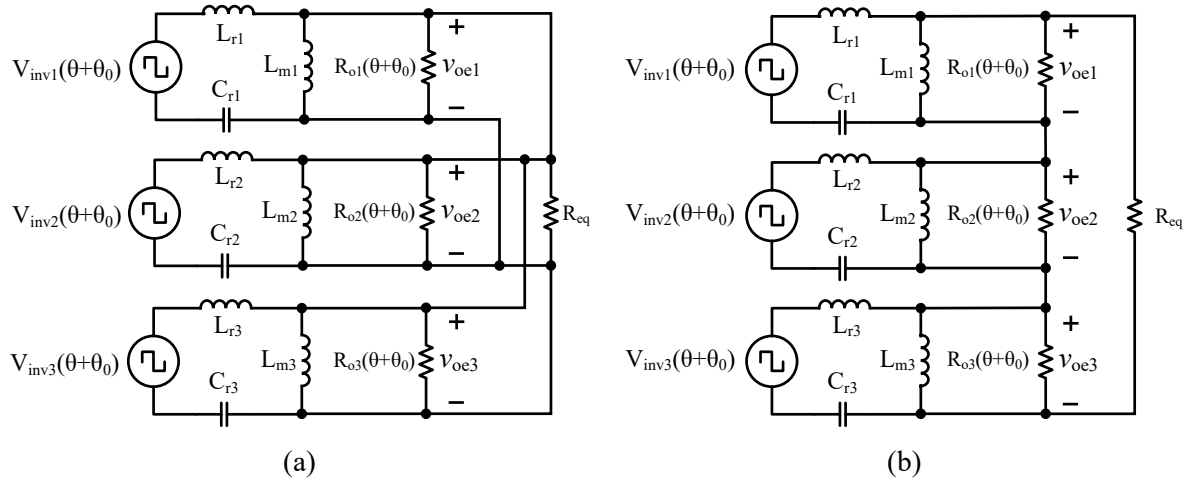

Fig. 3. The equivalent model of the three-phase AC-DC LLC converter, (a) Mode1, and (b) Mode 2.

Design considerations and control scheme

The first step in the design procedure of the proposed EV charger is to find the turn ratio of the transformer. It is important to make sure all the boundary output voltage conditions can be met. The detailed design of the single-stage PFC operation of three-phase soft-switching LLC-based rectifiers has been discussed in the literature [21] and [22]. The voltage range of the 400 V battery systems is considered to be from 250 V to 420 V and the voltage range of the 800 V battery systems is considered to be from 550 V to 850 V. To find out the transformer turn ratio, the minimum required gain by the rectifier at θ=90° is equal to the minimum available gain by the LLC converter. Please note that the maximum switching frequency swing will happen at the lowest output voltage condition of Mode 2 (i.e.,

a series connection of phase modules), which is for 550 V battery voltage. Hence, the output voltage range for each phase of the proposed EV charger should be designed from 550/3 V to 420 V. As the lower voltage limit for battery charging has a derating condition due to constant current charging, it is important to minimize circulating conduction losses for the voltages close to the rated battery voltage (e.g., 400 V and 800 V). Therefore, only for the 550 V condition, the switching frequency goes into an above series resonant region ($f_s < f_{sw}$) where a minimum required LLC voltage gain of 0.8 is realized. Hence, the turn ratio of the transformer ($n_{1,2,3} = N_{p1,2,3}/N_{s1,2,3}$) can be found in the following equations.

$$G_{req}{}^{min}(\theta) = \frac{V_{o1,2,3}{}^{min}}{V_{ac}} \rightarrow G_{req}{}^{min}(90°) = \frac{550/3}{V_{ac(pk)}} \tag{6}$$

$$G_{LLC(total)}{}^{min}(f_{sw}) = G_{LLC}{}^{min}(f_{sw}) \times \frac{1}{n_{1,2,3}} \rightarrow G_{LLC(total)}{}^{min}(f_{sw}) = \frac{0.8}{n_{1,2,3}} \tag{7}$$

$$G_{req}{}^{min}(\theta) = G_{LLC(total)}{}^{min}(f_{sw}) \rightarrow \frac{550/3}{V_{ac(pk)}} = \frac{0.8}{n_{1,2,3}} \rightarrow n_{1,2,3} = \frac{0.8 \times V_{ac(pk)}}{550/3} \tag{8}$$

Fig. 4 illustrates the design gain curves for the maximum and minimum switching frequency swing conditions, which is for V_o=550 V and V_o=420 V, respectively. It should be mentioned that this design is for a 1.5 kW prototype that was implemented in the laboratory. These design gain curves show the available gain curves for different line angles corresponding to different output power levels. The resonant tank parameters are designed such that the required minimum gain can be achieved for both boundary voltage conditions of each phase while minimizing the circulating current at the primary side of the LLC modules.

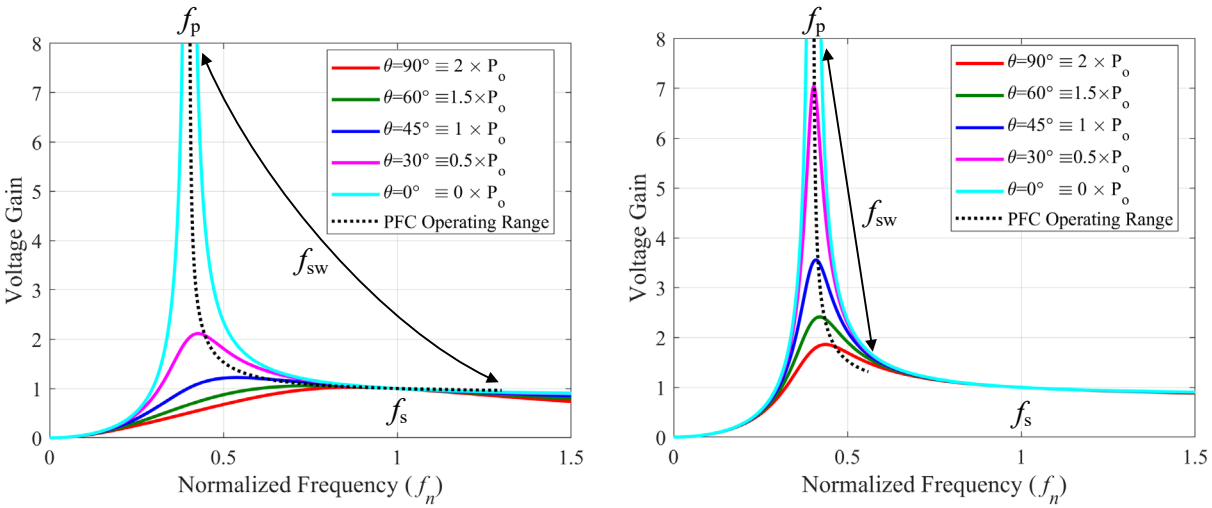

(a) V_o=550 V, P_o=1 kW, Mode 2 (b) V_o=420 V, P_o=1.5 kW, Mode 1

Fig. 4. LLC module design gain curves for (a) maximum switching frequency swing and (b) minimum switching frequency swing.

Fig. 5 illustrates a typical charging profile of both 400 V and 800 V battery systems with similar charging capacity being connected to the same power level EV charger. In the proposed EV charger, the maximum charging current is limited to I_{ch} for 400 V battery and it is limited to $I_{ch}/2$ for 800 V battery. Commonly, the first charging mode in battery charging is Constant Current (CC) followed by a Constant Voltage (CV) mode to maximize the battery State of Charge (SOC). The charging current at the end of a charging cycle is usually around 10 % of the CC charging current. It should be mentioned that in EV DC fast charging only the maximum deliverable power in CC mode is critical in order to increase the battery SOC from 10-20 % to 60-80 %. It should be mentioned that the DC fast charging profile can be

variable for different EVs to meet the temperature stress of the battery cells which is also dependent on the available battery cooling capacity.

The overall control scheme of the proposed EV charger is demonstrated in Fig. 6. In the control unit, the input three-phase voltages and currents are sensed to realize PFC, and the output voltage and current are sensed to realize the desired battery charging profile. Based on the pre-charging communication between the battery and the EV charger the proper signal for CC/CV charging and output mode selection of the proposed charger is decided to reflect the type, capacity, and SOC of the installed battery on the EV. Furthermore, three current reference signals are generated based on the sensed AC voltages that form three fast inner current loops for PFC. In the outer loop that is slower than the inner loops, the voltage/current feedback signals are compared with the reference signals and a control signal (v_c) is generated based on the desired charging mode that is then used in the inner current loops.

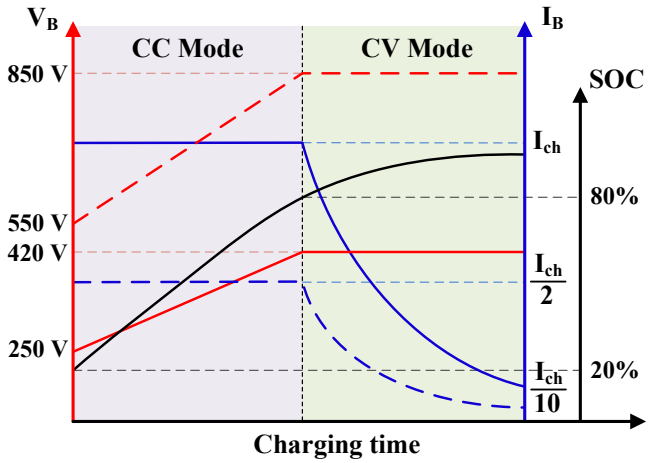

Fig. 5. The charging strategy of the proposed EV charger for both 400 V and 800 V batteries with similar capacity using the same power rating charger with a maximum current of I_{sh}.

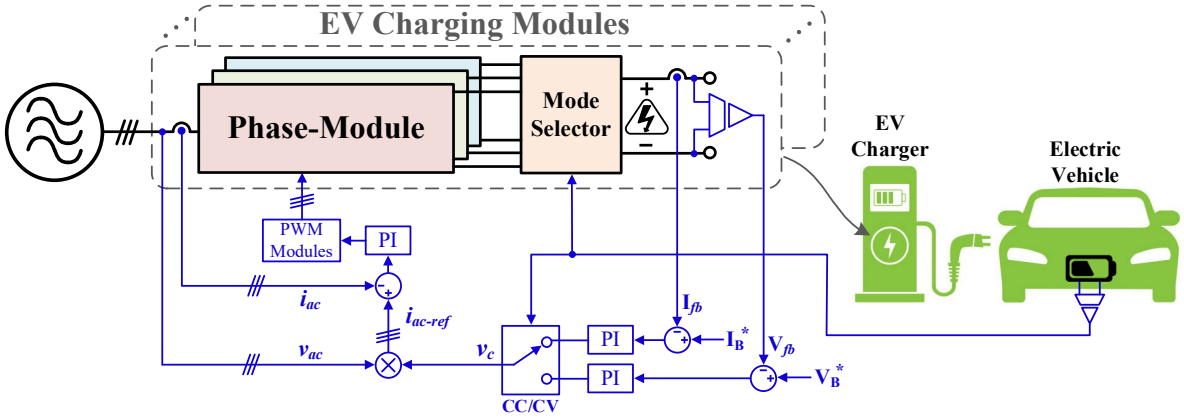

Fig. 6. The overall control scheme of the proposed wide output voltage range EV charger.

Simulation results

The proposed EV charger is simulated in the PSIM environment to verify its performance. Table I shows the design parameters used for both computer simulation and experiment. The resonant tank components are selected based on the design curves shown in Fig. 3 so all the operating conditions can be met. It should be mentioned that a small LC filter is used at the input of each module to filter the switching frequency ripple at the grid side. In the practical EV charging profile, around 30 % derating is considered for the depleted battery conditions, i.e., for 250 V in the 400 V battery and 550 V in the 800 V battery, and the full power should be available from V_o=320 V for 400 V battery system and from V_o=650 V for 800 V battery systems.

Table I: The parameters used in both simulation and experiment.

Parameters/Description		Values
Output Power Range (P_o)		1 kW - 1.5 kW
Input Voltages (V_a, V_b, V_c)		220 V_{ac}
Output Voltage Range (V_o)		250 V_{dc} - 850 V_{dc}
Switching Frequency Range ($f_{sw[1,2,3]}$)		200 kHz - 600 kHz
Parallel Resonant Inductor ($L_{m[1,2,3]}$)		120 µH
Series Resonant Inductor ($L_{r[1,2,3]}$)		22.5 µH
Series Resonant Capacitor ($C_{r[1,2,3]}$)		4.8 nF
Parallel Resonant Frequency (f_p)		191 kHz
Series Resonant Frequency (f_s)		484 kHz
Transformer Turns Ratio ($n_{[1,2,3]}$: 1)		1.35
Input LC Filter	Inductor ($L_{f[1,2,3]}$)	25 µH
	Capacitor ($C_{f[1,2,3]}$)	0.5 µF
Output Capacitor (C_{o1}, C_{o2}, C_{o3})		120 µF

Fig. 7. shows the steady-state line cycle simulation results for 400 V battery systems. For this condition, the output of the three-phase modules is connected in parallel. Fig. 7 (a) shows the simulation results for V_o=250 V. A scaled-down waveform of phase one's voltage is demonstrated to show a near unity power factor along with three-phase sinusoidal currents. As intended, the switching frequency of the three modules is close to the parallel resonant frequency around VZC points over the line cycle. Fig. 7 (b) shows the simulation results for V_o=420 V at rated output power. It can be observed that for the higher battery voltage condition also a unity power factor is achieved with near sinusoidal currents and low THD. Moreover, the output voltage ripple in both boundary conditions is below 100 mV.

The simulation results for the 800 V battery charging condition with series output connection of the three-phase modules are shown in Fig. 8. As can be observed from Fig. 8 (a) the switching frequency swing is from 200 kHz to 600 kHz for V_o=550 V which is in accordance with the design criteria mentioned in the previous section. Fig. 8 (b) illustrates the simulation results for V_o=850 V at rated output power. In both boundary conditions of the 800 V battery charging a unity power factor is achieved with a near sinusoidal current shape at the AC side. Furthermore, it can be observed that the output voltage of the proposed EV charger does not carry any low-frequency ripple in both parallel connection and series connection of the three-phase modules.

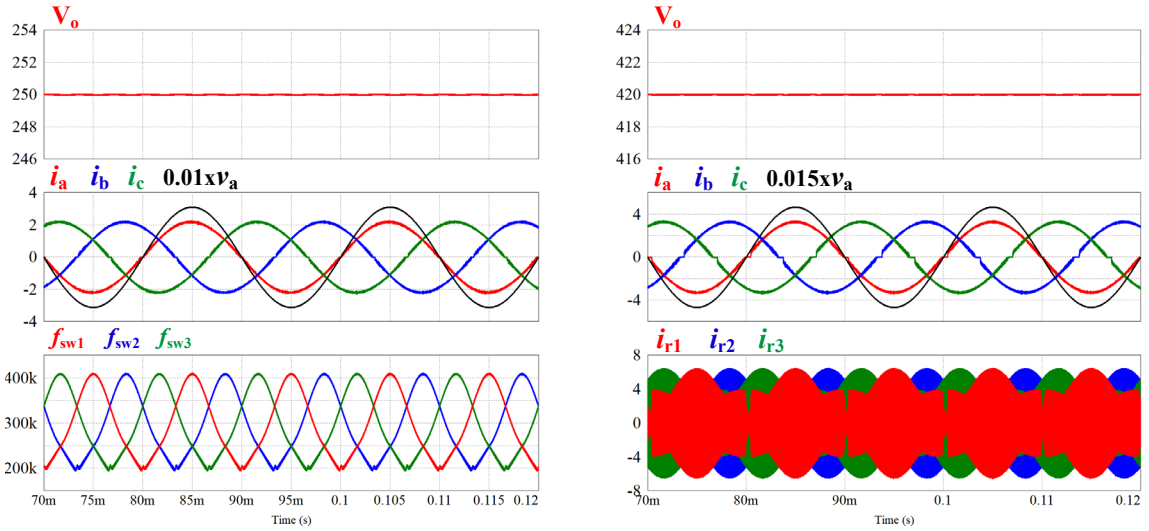

(a) V_o=250 V and P_o=1 kW (b) V_o=420 V and P_o=1.5 kW

Fig. 7. Line cycle simulation results for the 400 V battery charging profile.

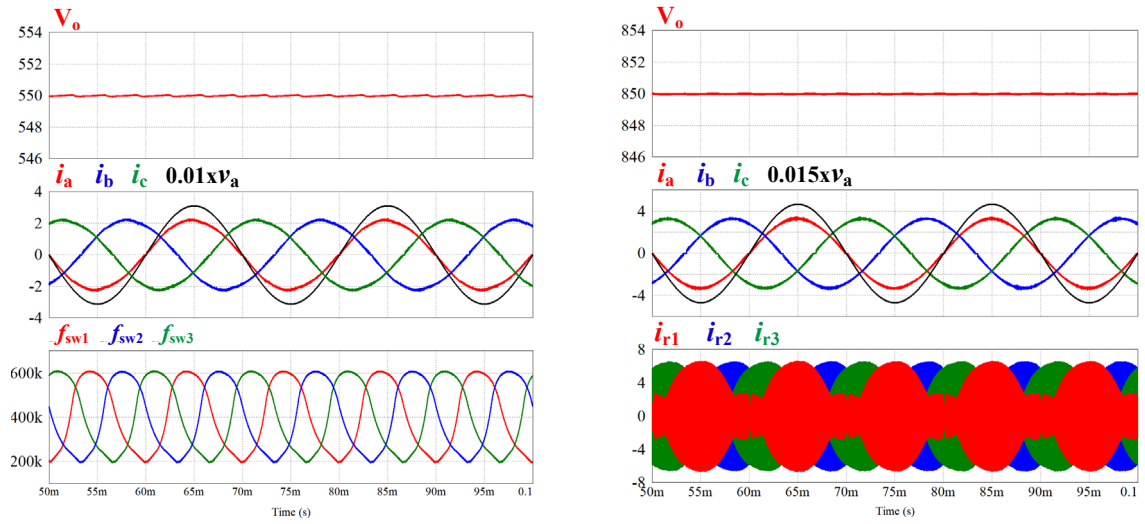

(a) V_o=550 V and P_o=1 kW (b) V_o=850 V and P_o=1.5 kW

Fig. 8. Line cycle simulation results for the 800 V battery charging profile.

Fig. 9 illustrates the simulation results of resonant current and magnetizing current for the peak power delivery condition in the positive line cycle (i.e., at θ=90°) for both minimum and maximum voltage levels of the 400 V and 800 V battery charging profiles. As can be observed from Fig. 9 (a), the operation of the LLC tank for 250 V output voltage is close to the series resonant frequency. The circulating current at the primary side of the transformer is 35 % in this condition. Fig. 8 (b) shows that the switching frequency for 420 V output voltage is far away from the series resonant frequency with the highest circulating current of 55 %. As expected from the design criteria shown in Fig. 4 (b), the switching frequency range is narrow for the 420 V condition. Fig. 9 (c) illustrates the minimum charging voltage for the series output connection in the 800 V battery charging profile with the maximum switching frequency operation and the circulating current of 18 % that is happening in the above resonant region. As demonstrated in Fig. 4 (a) the maximum switching frequency swing happens for the 550 V output voltage condition to reduce the RMS current and improve the circulating current for the 420 V output voltage condition. Fig. 9. (d) illustrates the maximum charging voltage condition with the switching frequency of 339 kHz and a 32 % circulating current.

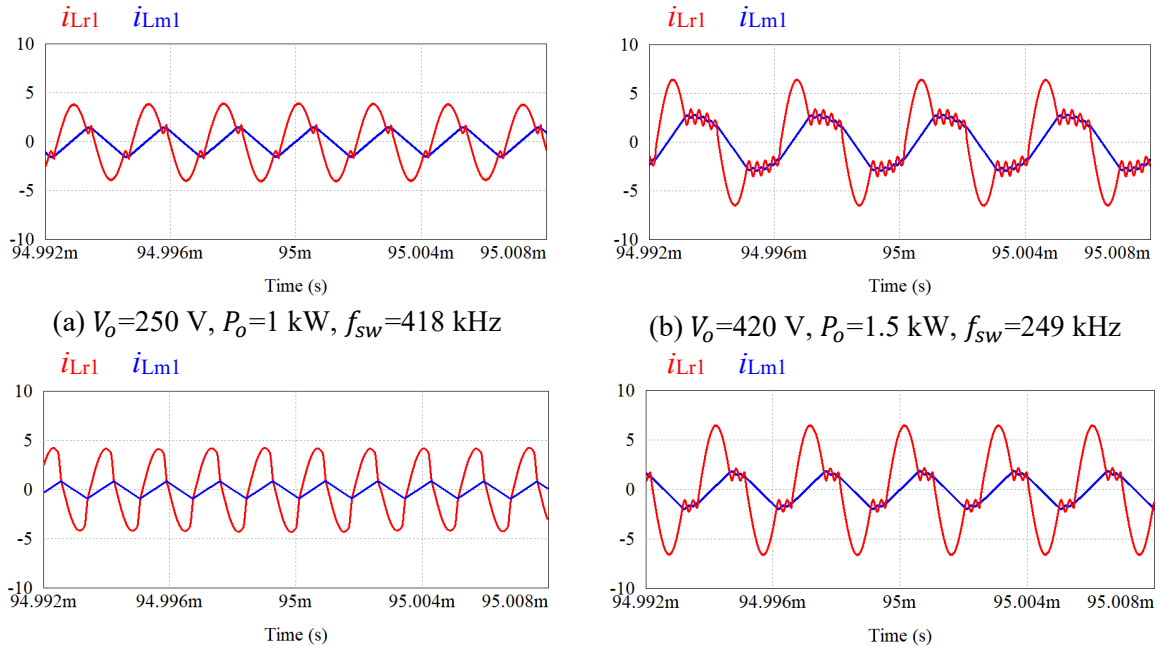

(a) V_o=250 V, P_o=1 kW, f_{sw}=418 kHz (b) V_o=420 V, P_o=1.5 kW, f_{sw}=249 kHz

(c) V_o=550 V, P_o=1 kW, f_{sw}=600 kHz (d) V_o=850 V, P_o=1.5 kW, f_{sw}=339 kHz

Fig. 9. Zoomed-in waveforms of peak power delivery at θ=90° for all boundary conditions of the 400 V and 800 V charging profiles.

Experimental results

A 1.5 kW prototype is built in the laboratory to verify the performance of the proposed EV DC fast charger. A single Microchip dsPIC microcontroller is used to perform digital control implementation of the proposed three-phase charger. In the MCU, a look-up table is used to implement the reference signals for the three-phase input current to realize a proper PFC. It should be mentioned that in the prototype the input diode rectifiers are 650 V Silicon diodes and 650 V GaN HEMTs are used for the primary switching bridges while 650 V SiC diodes are used for the output rectifiers of each module. Hence, all the switching devices of the proposed EV DC fast charger are rated for 650 V, which increases the reliability while keeping the implementation costs down.

Fig. 10 (a) shows the experimental result for three-phase currents over the line frequency for the 420 V output voltage condition. In this case, double pole relays in Fig. 2 are in position 1 so the output of the three-phase modules are connected in parallel. As can be observed, a proper PFC is achieved in all phases and the output voltage does not consist of any low-frequency ripple. Fig. 10 (b) shows the line frequency experimental results for the 850 V output voltage condition. In this case, the double pole relays are set in position 2 so the output of the three-phase modules is connected in series.

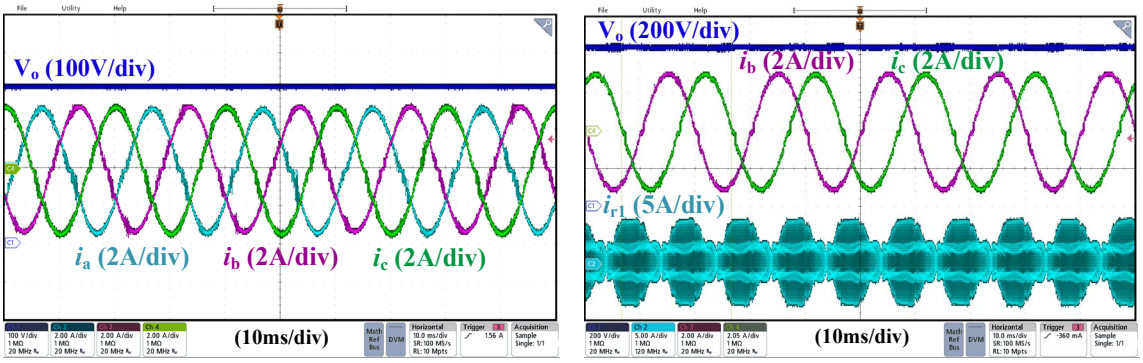

(a) V_o=420 V and P_o=1.5 kW (b) V_o=850 V and P_o=1.5 kW

Fig. 10. Line cycle experimental results of the proposed EV charger for both battery voltage levels.

The zoomed-in resonant current waveforms are shown in Fig. 11 for both 420 V and 850 V output voltage conditions. The maximum switching frequency that happens at θ=90° is 240 kHz for V_o=420 V and the maximum switching frequency for V_o=850 V is equal to 337 kHz. Both conditions are as expected and according to the simulation results shown in Fig. 7 to Fig. 9.

The efficiency measurements for V_o=420 V - P_o=1.5 kW shows around 96.5 % efficiency and for V_o=850 V - P_o=1.5 kW shows around 96.2 % efficiency. It should be mentioned that based on power loss estimations the efficiency can be improved by around 1 % after changing the input rectifiers with Si MOSFETs and using SiC MOSFETs for the synchronous rectifiers.

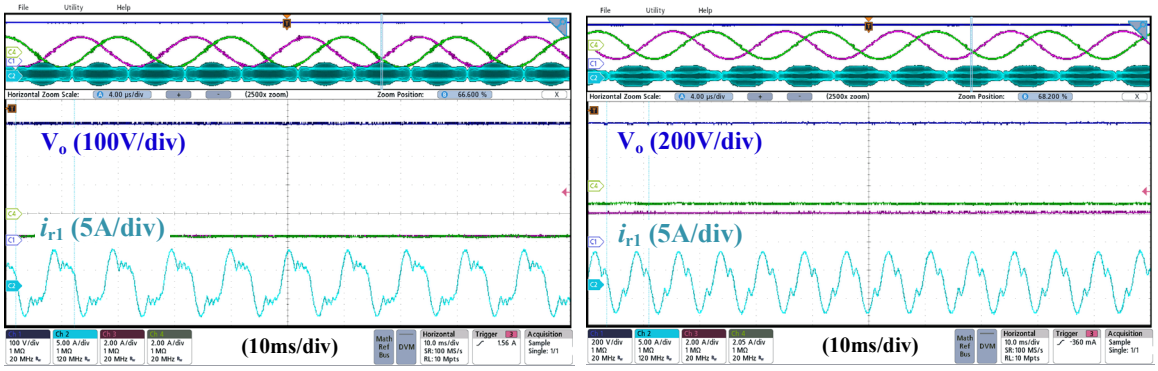

(a) V_o=420 V, P_o=1.5 kW and f_{sw}=240 kHz (b) V_o=850 V, P_o=1.5 kW and f_{sw}=337 kHz

Fig. 11. Zoomed-in resonant current waveforms of different battery pack voltage levels.

Conclusion

A new single-stage three-phase EV charger with reconfigurable output has been proposed in this paper. The main characteristics of the proposed EV charger include soft-switching, no dc-link capacitor requirement, and suitability for both 400 V and 800 V automotive battery systems. The analysis demonstrated a suitable resonant tank design for a wide output voltage operation in the proposed three-phase EV DC fast charger. Computer simulation results verified the proper PFC performance and small output voltage ripple of the proposed single-stage three-phase EV charger over a wide output voltage range from 250 V to 850 V. Moreover, a 1.5 kW laboratory prototype has been built to verify the practicability of the proposed EV DC fast charger for both 400 V and 800 V battery charging applications.

References

[1] O. Ellabban, H. Abu-Rub and F. Blaabjerg. "Renewable energy resources: Current status, future prospects and their enabling technology." *Renewable Sustain. Energy Rev.,* vol 39, pp. 748-764, 2014.

[2] B. Wang, M. Xu and L. Yang. "Study on the economic and environmental benefits of different EV powertrain topologies." *Energy Convers. Manage.,* vol 86, pp. 916-926, 2014.

[3] M. Pahlevani and P. K. Jain, "Soft-Switching Power Electronics Technology for Electric Vehicles: A Technology Review," *IEEE J. Emerg. Sel. Topics Ind. Electron.*, vol. 1, no. 1, pp. 80-90, July 2020.

[4] S. Chon, M. Bhardwaj and H. Nene. "Maximizing power for Level 3 EV charging stations." *Texas Instrument Article*, pp. 1-33, 2018.

[5] Y. Li, J. Schäfer, D. Bortis, J. W. Kolar and G. Deboy, "Optimal Synergetic Control of a Three-Phase Two-Stage Ultra-Wide Output Voltage Range EV Battery Charger Employing a Novel Hybrid Quantum Series Resonant DC/DC Converter," in *Proc. IEEE 21st Workshop on Control and Modeling for Power Electronics (COMPEL)*, pp. 1-11, 2020.

[6] M. Leibl, J. W. Kolar and J. Deuringer, "Sinusoidal Input Current Discontinuous Conduction Mode Control of the VIENNA Rectifier," *IEEE Trans. Power Electron.*, vol. 32, no. 11, pp. 8800-8812, Nov. 2017.

[7] C. Lim, Y. Jeong, M. Lee, K. Yi and G. Moon, "Half-Bridge Integrated Phase-Shifted Full-Bridge Converter With High Efficiency Using Center-Tapped Clamp Circuit for Battery Charging Systems in Electric Vehicles," *IEEE Trans. Power Electron.*, vol. 35, no. 5, pp. 4934-4945, May 2020.

[8] C.-C. Hua, Y.-H. Fang and C.-W. Lin. "LLC resonant converter for electric vehicle battery chargers." *IET Power Electron.,* vol. 9. no. 12, pp. 2369-2376, 2016.

[9] M. Forouzesh and Y. -F. Liu, "Interleaved LCLC Resonant Converter With Precise Current Balancing Over a Wide Input Voltage Range," *IEEE Trans. Power Electron.*, vol. 36, no. 9, pp. 10330-10342, Sept. 2021.

[10] D. Das, N. Weise, K. Basu, R. Baranwal and N. Mohan, "A Bidirectional Soft-Switched DAB-Based Single-Stage Three-Phase AC–DC Converter for V2G Application," *IEEE Trans. Transport. Electrific.*, vol. 5, no. 1, pp. 186-199, March 2019.

[11] N. Rathore, S. Gangavarapu, A. K. Rathore and D. Fulwani, "Emulation of Loss Free Resistor for Single-Stage Three-Phase PFC Converter in Electric Vehicle Charging Application," *IEEE Trans. Transport. Electrific.*, vol. 6, no. 1, pp. 334-345, March 2020.

[12] T. Mishima and S. Mitsui, "A Single-Stage High Frequency-link Modular Three-Phase Soft-Switching AC-DC Converter for EV Battery Charger," in *Proc. IEEE Energy Conversion Congress and Exposition (ECCE)*, 2019, pp. 2141-2147.

[13] V. Reber. (2016). *E-Power: New Possibilities With 800-Volt Charging.* Porsche Eng. Mag. Accessed: Dec. 2021. [Online]. Available: https://www.porscheengineering.com/peg/en/about/magazine/

[14] C. Jung, "Power Up with 800-V Systems: The benefits of upgrading voltage power for battery-electric passenger vehicles," *IEEE Electrific. Mag.*, vol. 5, no. 1, pp. 53-58, March 2017.

[15] I. Aghabali, J. Bauman, P. J. Kollmeyer, Y. Wang, B. Bilgin and A. Emadi, "800-V Electric Vehicle Powertrains: Review and Analysis of Benefits, Challenges, and Future Trends," *IEEE Trans. Transport. Electrific.*, vol. 7, no. 3, pp. 927-948, Sept. 2021.

[16] M. Abbasi and J. Lam, "An SiC-Based AC/DC CCM Bridgeless Onboard EV Charger With Coupled Active Voltage Doubler Rectifiers for 800-V Battery Systems," in *Proc. IEEE Applied Power Electronics Conference and Exposition (APEC)*, 2020, pp. 905-910.

[17] S. Sen, L. Zhang, T. Chen, J. Zhang and A. Q. Huang, "Three-phase Medium Voltage DC Fast Charger based on Single-stage Soft-switching Topology," in *Proc. IEEE Transportation Electrification Conference and Expo (ITEC)*, 2018, pp. 1123-1128.

[18] J. -Y. Kim, B. -S. Lee, D. -H. Kwon, D. -W. Lee and J. -K. Kim, "Low Voltage Charging Technique for Electric Vehicles With 800 V Battery," *IEEE Trans. Ind. Electron.*, doi: 10.1109/TIE.2021.3109526. (Early Access)

[19] G. V. Bharath, S. Kiran Voruganti, V. T. Nguyen, V. Uttam Pawaskar and G. Gohil, "Performance Evaluation of 10kV SiC-based Extreme Fast Charger for Electric Vehicles with Direct MV AC Grid Interconnection," in *Proc. IEEE Applied Power Electronics Conference and Exposition (APEC)*, 2020, pp. 3547-3554.

[20] W. Liu, A. Yurek, B. Sheng, Y. Chen, Y. -F. Liu and P. C. Sen, "A Single Stage 1.65kW AC-DC LLC Converter with Power Factor Correction (PFC) for On-Board Charger (OBC) Application," in *Proc. IEEE Energy Conversion Congress and Exposition (ECCE)*, 2020, pp. 4594-4601.

[21] M. Forouzesh, Y. -F. Liu and P. C. Sen, "Implementation of an Isolated Phase-Modular-Designed Three-Phase PFC Rectifier Based on Single-Stage LLC Converter," in *Proc. IEEE Energy Conversion Congress and Exposition (ECCE)*, 2021, pp. 2266-2273.

[22] M. Forouzesh, Y. -F. Liu and P. C. Sen, "A Novel Soft-Switched Three-Phase Three-Wire Isolated AC-DC Converter With Power Factor Correction," in *Proc. IEEE Applied Power Electronics Conference and Exposition (APEC)*, 2022, pp. 887-894.